

Analytical Expression of the Magnetic Field Created by a Permanent Magnet with Diametrical Magnetization

Van Tai Nguyen* and Tien-Fu Lu

Abstract—Cylindrical/ring-shaped permanent magnets with diametrical magnetization can be found in many applications, ranging from electrical motors to position sensory systems. In order to correctly calculate the magnetic field generated by a permanent magnet of this kind with low computational cost, several studies have been reported in literature providing analytical expressions. However, these analytical expressions are either limited for an infinite cylinder or for computing the magnetic field only on the central axis of a finite cylinder. The others are derived to calculate the magnetic field at any point in three-dimensional (3D) space but only with low accuracy. This paper presents an exact analytical model of the magnetic field, generated by a diametrically magnetized cylindrical/ring-shaped permanent magnet with a limited length, which can be used to calculate the magnetic field of any point in 3D space fast and with very high accuracy. The expressions were analytically derived, based on geometrical analysis without calculating the magnetic scalar potential. Also, there is no approximation in the derivation steps that yields the exact analytical model. Three components of the magnetic field are analytically represented using complete and incomplete elliptical integrals, which are robust and have low computational cost. The accuracy of the developed analytical model was validated using Finite Element Analysis and compared against existing models.

1. INTRODUCTION

Permanent magnets have been widely utilised in various applications [1–10]. Amongst them, cylindrical and ring shaped permanent magnets with diametrical magnetization have been widely used in electrical motors [11–14] and in position sensory systems [15–18] including human intention recognition [19]. The requirement for an accurate and fast-computed analytical expression of the magnetic field generated by a diametrically magnetised permanent magnet that can facilitate the design optimization of magnetic devices and modelling dynamical systems [20, 21], leads to various ways of expressing the magnetic field of a permanent magnet of this kind. Since it can be time-consuming to use Finite Element Method, analytical expressions with minimal computational effort have been attracting attention. This is very useful, especially when modelling dynamic systems, such as the movement of magnetic nanoparticles in a magnetic field gradient [22]. Moreover, a fast-computed analytical expression of the magnetic field can help save computational time to solve an optimization problem with variations over a large number of parameters [23].

Currently, based on elliptic integral functions, three dimensional (3D) analytical expressions of the magnetic field created by a permanent magnet with radial and axial magnetization have been derived [24, 25]. For these magnets, the surface charge density is constant. However, in the case of a diametrically magnetised permanent magnet, this parameter is dependent on the angle φ between the magnetization vector \vec{J} and the normal unit vector \vec{n} to the cylindrical surface which is equal to $J \cos \varphi$ [22]. Therefore, the nonconstant surface charge density needs to be taken into account

Received 30 July 2018, Accepted 28 September 2018, Scheduled 9 October 2018

* Corresponding author: Van Tai Nguyen (vantai.nguyen@adelaide.edu.au).

The authors are with the School of Mechanical Engineering, University of Adelaide, SA 5005, Australia.

when deriving the analytical expressions of the magnetic field generated by a permanent magnet with diametrical magnetization. There are some analytical expressions of the magnetic field produced by a diametrically magnetised permanent magnet. However, they are developed only for an infinite cylinder [26, 27], or for computing the magnetic field only on the central axis of a finite cylinder [28]. In order to address these limitations, most recently, Caciagli et al. [22] presented an analytical model, based on complete elliptic integrals, to calculate the magnetic field created by a diametrically magnetised cylindrical permanent magnet with a finite length, at any point in (3D) space. Nonetheless, in the steps of derivation, the scalar potential is approximately expressed with the complete elliptic integrals; this caused an error associated with the final expressions of the magnetic field, because these final expressions were derived by taking the derivatives of the approximated scalar potential directly. This error is demonstrated in this paper under Section 3, Finite Element verification and discussion. Fontana et al. [29] presented the double integration expression, which can be used to calculate the magnetic field created by a permanent magnet with diametrical magnetization at any point of interest in 3D space. However, the double integration expression can be solved only numerically that can be time-consuming when high accuracy needs to be achieved.

To eliminate/reduce the aforementioned error due to the approximation and improve the computation costs, this paper presents the work leading to an exact analytical expression of the magnetic field created by a diametrically magnetised cylindrical- and ring-shaped permanent magnet at any point of interest in 3D space, based on the Coulombian approach [30] which has been used to analytically model the magnetic fields created by arc-shaped permanent magnets with radial magnetization [31, 32], ring-shaped permanent magnets with axial and radial magnetization [24, 33], tile permanent magnets with radial magnetization [25] and tangential magnetization [34, 35]. The exact final model of the magnetic field was analytically derived, based on geometrical analysis without the need to calculate the scalar potential; and there was no approximation in the derivation steps. All three components of the magnetic field can be expressed using complete and incomplete elliptic integrals that are robust and their computational efforts are minimal [22, 36–39]. The accuracy of the developed analytical model was validated against 3D FEA results.

The rest of this paper is organised as follows. Section 2 presents the mathematical derivation of the analytical expressions of the axial, azimuthal and radial components of the magnetic field generated by a cylindrical/ring shaped permanent magnet with diametrical magnetization. Section 3 compares the results of the developed model with those of Finite Element Analysis and with those of the existing model recently derived by Caciagli et al. [22]. Section 4 draws the conclusions.

The MATLAB codes of the derived analytical expressions in this paper will be made available in public domain for readers to use once the manuscript is accepted for publication. The codes will be published in the authors' profiles on www.researchgate.net and on the authors' Adelaide University profile pages.

2. MATHEMATICAL DERIVATION

A diametrically magnetized cylindrical permanent magnet with parameters is illustrated in Figs. 1(a) and (b); its radius is R ; its thickness is h ; its magnetization \vec{J} is assumed to be uniformly diametrical and along axis Y .

The derivations are based on the Coulombian model in a cylindrical coordinate system (r, α, z) with an azimuth coincident with axis X (Fig. 1(a)). According to the Coulombian model, the magnetic field intensity at any observation point K (Fig. 1) produced by a permanent magnet in the 3D space can be expressed as follows [31]:

$$\vec{H}_K = \frac{1}{4\pi\mu_0} \left(\iint_s \frac{\sigma_s}{|\vec{i}-\vec{i}'|^3} (\vec{i}-\vec{i}') ds + \iiint_v \frac{\sigma_v}{|\vec{i}-\vec{i}'|^3} (\vec{i}-\vec{i}') dv \right) \quad (1)$$

The volume charge can be defined as $\sigma_v = -\vec{\nabla} \cdot \vec{J}$ the divergence of the magnetization vector \vec{J} is equal to zero because it is uniformly diametrical; hence, the magnetic field intensity can be calculated using only the surface charge component, which is the first part of equation in the larger parentheses of Eq. (1).

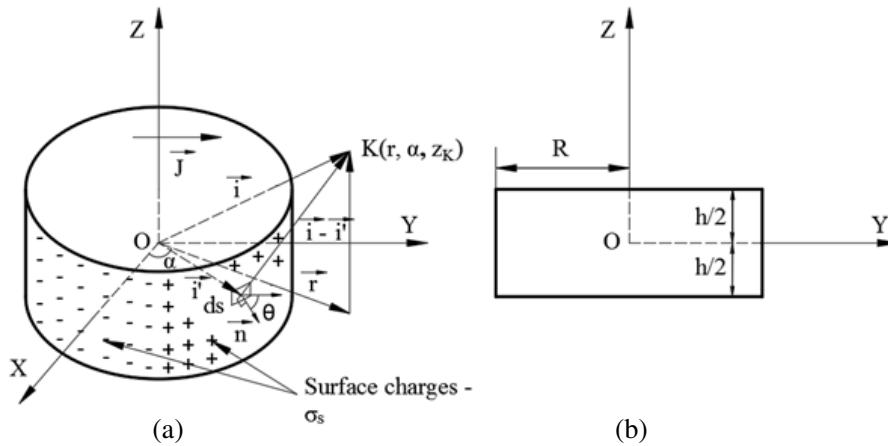


Figure 1. Diametrically magnetized cylindrical permanent magnet; (a) Isometric view and (b) front view.

The surface charge can be calculated as $\sigma_s = \vec{J}\vec{n} = J \cos \theta = J \sin(\alpha + \beta)$; here θ is the angle between the magnetization vector \vec{J} and the normal unit vector \vec{n} to the cylindrical surface (Fig. 1(a)), α is the azimuthal angle and $\beta = \pi/2 - \theta - \alpha$.

After taking the projection of $(\vec{i} - \vec{i}')$ on the radial, azimuthal and axial directions ($\vec{i}_r, \vec{i}_\alpha$ and \vec{i}_z are the unit vectors respectively), with the consideration that the volume charge has no contribution to the magnetic field, Eq. (1) can be rewritten in the double integration form as follows [29]:

$$\vec{H}_K = \frac{JR}{4\pi\mu_0} \int_{\beta=-\pi}^{\beta=\pi} \int_{z=-\frac{h}{2}}^{z=\frac{h}{2}} \frac{(r - R \cos \beta) \vec{i}_r + (-R \sin \beta) \vec{i}_\alpha + (z_K - z) \vec{i}_z}{(R^2 + r^2 - 2Rr \cos \beta + (z_K - z)^2)^{\frac{3}{2}}} \sin(\alpha + \beta) dz d\beta \quad (2)$$

After analytically integrating each component of the magnetic field along the axial, azimuthal and radial directions in Eq. (2), the analytical expressions of the axial, azimuthal and radial components of the magnetic field were obtained as follows:

2.1. The Axial Component

Table 1. Parameters used in Eq. (3).

Parameters	Definition
a	$(z_K - \frac{h}{2})^2 + R^2 + r^2$
b	$(z_K + \frac{h}{2})^2 + R^2 + r^2$
c	$2Rr$
p	$\frac{2c}{c-a}$
u	$\frac{2c}{c-b}$

The analytical expression of the axial component $H_{K(z)}^{(3D)}(r, \alpha, z_K)$ was obtained with the parameters illustrated in Table 1:

$$H_{K(z)}^{(3D)}(r, \alpha, z_K) = \frac{JR \sin \alpha}{\pi\mu_0} \left(\frac{(a\mathbf{K}[p] + (c-a)\mathbf{E}[p])}{c\sqrt{a-c}} - \frac{(b\mathbf{K}[u] + (c-b)\mathbf{E}[u])}{c\sqrt{b-c}} \right) \quad (3)$$

$$\text{Here, } \mathbf{K}[m] = \int_0^{\frac{\pi}{2}} \frac{d\theta}{\sqrt{1 - m\sin^2\theta}} \text{ is the complete elliptic integral of the first kind,} \quad (3a)$$

$$\mathbf{E}[m] = \int_0^{\frac{\pi}{2}} \sqrt{1 - m\sin^2\theta} \text{ is the complete elliptic integral of the second kind.} \quad (3b)$$

2.2. The Azimuthal Component

Table 2. Parameters used in Eq. (4) and Eq. (5).

Parameters	Definition
a	$R^2 + r^2$
b	$2Rr$
c	$\frac{h}{2} - z_K$
d	$\frac{h}{2} + z_K$
t	$\cos \beta$
ζ	$\sqrt{1 - t^2}$
η	$\sqrt{\frac{b(t+1)}{a+b+c^2}}$
κ	$\sqrt{\frac{b(t-1)}{a-b+c^2}}$
λ	$\sqrt{\frac{a-bt+c^2}{a+b+c^2}}$
ν	$\text{ArcSin} \left[\frac{\sqrt{t+1}}{\sqrt{2}} \right]$
ξ	$\frac{2b}{c^2+a+b}$
ς	$\frac{2b}{a+b}$
χ	$\text{ArcSin} \left[\sqrt{\frac{c^2+a-bt}{c^2+a+b}} \right]$
ψ	$\frac{c^2+a+b}{c^2+a-b}$
Υ	$\frac{4r^2}{c^2+4r^2}$

The analytical expression of the tangential component $H_{K(\alpha)}^{(3D)}(r, \alpha, z_K)$ was obtained with the parameters illustrated in Table 2 as follows:

$$H_{K(\alpha)}^{(3D)}(r, \alpha, z_K) = \frac{JR^2 \cos \alpha}{2\pi\mu_0} (\delta(t_2, a, b, c) - \delta(t_1, a, b, c) + \delta(t_2, a, b, d) - \delta(t_1, a, b, d)) \quad (4)$$

where, the auxiliary function δ is as follows:

$$\delta(t, a, b, c) = -\frac{2c\lambda}{b^2\zeta\sqrt{a-bt+c^2}} (-a\zeta\mathbf{F}[\nu, \xi] + (a-b)\zeta\mathbf{Pi}[\varsigma, \nu, \xi] + (t+1)b\kappa\mathbf{F}[\chi, \psi] + (t+1)(-(-a+b-c^2))\kappa\mathbf{E}[\chi, \psi]);$$

$$\text{Here, } \mathbf{F}[\varphi, m] = \int_0^\varphi \frac{d\theta}{\sqrt{1 - m\sin^2\theta}} \text{ is the incomplete elliptic integral of the first kind,} \quad (4a)$$

$$\mathbf{E}[\varphi, m] = \int_0^\varphi \sqrt{1 - m\sin^2\theta} \text{ is the incomplete elliptic integral of the second kind,} \quad (4b)$$

$$\mathbf{Pi}[n, \varphi, m] = \int_0^\varphi \frac{d\theta}{(1 - n\sin^2\theta)\sqrt{1 - m\sin^2\theta}} \text{ is the incomplete elliptic integral of the third kind.} \quad (4c)$$

2.3. The Radial Component

The analytical expression of the radial component $H_{K(r)}^{(3D)}(r, \alpha, z_K)$ was obtained with parameters as illustrated in Table 2 as follows:

$$H_{K(r)}^{(3D)}(r, \alpha, z_K) = \frac{JR \sin \alpha}{2\pi\mu_0} (\gamma(t_2, a, b, c, r, R) - \gamma(t_1, a, b, c, r, R) + \gamma(t_2, a, b, d, r, R) - \gamma(t_1, a, b, d, r, R)) \quad (5)$$

where, the auxiliary function γ is as follows:

$$\gamma(t, a, b, c, r, R) = (2c\lambda ((a+b)(a-b+c^2)R\kappa(1+t)\mathbf{E}[\chi, \psi] + (a+b)(br-aR)\eta\zeta\mathbf{F}[\nu, \xi] + (a+b+at+bt)bR\kappa\mathbf{F}[\chi, \psi] + (aR-br)a\eta\zeta\mathbf{Pi}[\varsigma, \nu, \xi]) / (\eta\zeta b^2(a+b)\sqrt{a+c^2-bt});$$

For the point K on the cylindrical surface, or when $r = R$, the radial component can be calculated as follows:

$$H_{K(r)}^{(3D)}(r = R, \alpha, z_K) = \frac{J \sin \alpha}{4\pi\mu_0} (cf(r, c) + df(r, d)) \quad (5a)$$

where, the auxiliary function f is expressed as follows:

$$f(r, c) = \frac{(c^2+2r^2)\mathbf{K}[\Upsilon] - (c^2+4r^2)\mathbf{E}[\Upsilon]}{r^2\sqrt{c^2+4r^2}}$$

The complete elliptic integrals of the first and second kinds \mathbf{K} [m], \mathbf{E} [m] are calculated using Eq. (3a) and Eq. (3b).

The incomplete elliptic integrals of the first, second and third kinds \mathbf{F} , \mathbf{E} and \mathbf{Pi} are calculated using Eqs. (4a), (4b) and (4c).

The values of t_1 and t_2 in Eq. (4) and Eq. (5) can be set to be 0.999999999 or closer to 1 and -0.999999999 or closer to -1 respectively to avoid indefinite values whilst evaluating the expressions.

2.4. Calculation of the Magnetic Field Created by a Diametrically Magnetized Ring Shaped Permanent Magnet

For a ring shaped permanent magnet with the parameters shown in Fig. 2, its inner radius is R_{in} ; its outer radius is R_{out} ; its thickness is h ; its magnetization \vec{J} is assumed to be uniformly diametrical and along axis Y ; the magnetic field $\vec{H}_K(\text{ring})$ at point K can be computed using the principle of superposition Eq. (6):

$$\vec{H}_K(\text{ring}) = \vec{H}_K(R_{out}) - \vec{H}_K(R_{in}) \quad (6)$$

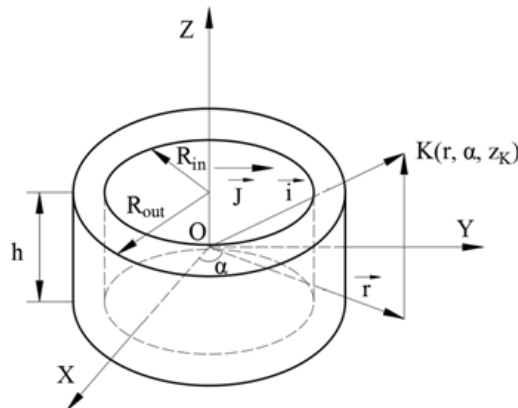


Figure 2. Diametrically magnetized ring shaped permanent magnet.

where $\vec{H}_K(R_{out})$ is the magnetic field at point K created by a cylinder with the radius R_{out} , and $\vec{H}_K(R_{in})$ is the magnetic field at point K created by another cylinder with the radius R_{in} . These two cylinders have the same \vec{J} and thickness as those of the ring. Using the above expressions from Eq. (3) to Eq. (6), the axial, azimuthal and radial components of the magnetic field of a diametrically magnetized ring shaped permanent magnet can be calculated.

Knowing the magnetic field intensity, the magnetic flux density can be computed as follows:

$$\vec{B}_K = \mu_0 \vec{H}_K \quad (\text{in the air space}) \quad (7)$$

$$\text{and } \vec{B}_K = \mu_0 \vec{H}_K + \vec{J} \quad (\text{inside the magnet}) \quad (8)$$

3. FINITE ELEMENT VERIFICATION AND DISCUSSION

The developed analytical expressions were implemented in MATLAB R2016b of MATHWORKS to calculate the axial, azimuthal and radial components of the magnetic flux density, both in the air space and inside the magnet, generated by a cylinder diametrically magnetised rare earth permanent magnet (Fig. 1) with a radius $R = 2.5$ mm and thickness $h = 5$ mm; and magnetic remanence $J = 1$ T, which is generated by a scalar coercivity of $800000 \text{ A}\cdot\text{m}^{-1}$ [22]. The Finite Element Analysis was carried out using Electromagnetic simulation software (EMS) from EMWORKS and integrated with 3D CAD INVENTOR software from AUTODESK.

The error between the results of the analytical expressions ($B_{\text{Analytical}}$) and those of the Finite Element (FE) model ($B_{\text{FE model}}$) is calculated using Eq. (9)

$$\text{Error} = \left| \frac{B_{\text{Analytical}} - B_{\text{FE model}}}{B_{\text{FE model}}} \right| \times 100\% \quad (9)$$

In Figs. 3(a), 4(a) and 5(a), the magnetic field components are presented with a solid line for those computed using the derived analytical expressions of this paper, with circles for those computed using the FE model and with a dotted line for those computed using the model by Caciagli et al. [22]. In Figs. 3(b), 4(b) and 5(b), the errors are presented with a solid line for those of the derived analytical expression of this paper, and with a dashed line for those of the Caciagli et al. model [22].

Figures 3(a) and (b) show that the developed analytical expressions can compute the magnetic field precisely, with an average error of less than 2.5% for the axial component inside the magnet, except for the field point near the centre of the cylinder (the radial distance r is less than 1 mm) where the

Table 3. Errors of the analytical model derived in this paper and those of Caciagli et al. [22] tested against the Finite Element (FE) model with r in the interval from 0 mm to 12.5 mm: * denotes the errors inside the magnet, ** denotes the errors in the air space.

Components of the magnetic field	Maximum error (%)				Average error (%)				Minimum error (%)			
	Model derived in this paper		Model by Caciagli et al. [22]		Model derived in this paper		Model by Caciagli et al. [22]		Model derived in this paper		Model by Caciagli et al. [22]	
	*	**	*	**	*	**	*	**	*	**	*	**
Axial component	28.9	5.4	916.5	154	less than 2.5	less than 2	362.2	97.9	0.068	0.16	47.1	39.1
Azimuthal component	0.16	3.36	828.5	254.9	less than 0.16	less than 1.5	249.4	112	0.007	0.49	24.04	34.24
Radial component	0.2	1.8	819.7	174.3	less than 0.2	less than 1.5	237.8	91.2	0.005	0.002	2.6	47.67

Table 4. Computational times.

Components of the magnetic field	Time-consumption (seconds)		
	Double integration model [29]	Analytical model in this paper	Analytical model by Caciagli et al. [22]
Axial component	0.33	4.6×10^{-3}	0.08×10^{-3}
Azimuthal component	0.045	0.15	0.018
Radial component	0.24	0.15	0.018
Total	0.615	0.3046	0.03608

Table 5. Comparison of the axial component of the magnetic field computed by the analytical model derived in this paper and those of double integration form [29].

Computed points K (r mm, α° , z mm)	Analytical model in this paper	Double integration model [29]
(1, 30°, 1)	$2.157769964794315e + 02$	$2.157769964794310e+02$
(2, 60°, 1)	$6.708086824080323e + 02$	$6.708086824080297e+02$
(2, 90°, 2)	$2.090489643938749e + 03$	$2.090489643938752e+03$
(3, 60°, 2)	$1.642034971824546e + 03$	$1.642034971824547e+03$
(7, 45°, 3)	$1.285267148068441e + 02$	$1.285267148068443e+02$
(8, 45°, 2)	64.672428644072369	64.672428644071971
(9, 0°, 3)	0	$-1.663901291691562e - 14$ when the integration increment increased to square root of the minimum; indefinite with the minimum integration increment

error is up to 30%; this could be due to the mesh-based approach of the finite-element solver [22], for example, the mesh could not be fine enough to yield exact results such as some nodes of the calculated point were located in the negative field when the point is close to the centre of the cylinder. The average error decreases to below 2% in the air space and it continues to decline with the increase of the radial distances. In contrast, the model developed by Caciagli et al. [22] yields inaccurate result with a minimum error of 39.1% and this error increases for the other field points inside the magnet and in the air space. Figs. 4 and 5 show that using the derived analytical expressions, the average errors are lower than 0.2% for the azimuthal and radial components inside the magnet. The errors increase for the magnetic field close to the cylindrical surface of the magnet ($r \approx R$), where a discontinuity of the magnetic field is observed (Fig. 4(a) and Fig. 5(a), the discontinuity value of the radial component can be calculated using Eq. (5a)). This is, however as mentioned before, due to the mesh-based approach

Table 6. Comparison of the azimuthal component of the magnetic field computed by the analytical model derived in this paper and those of double integration form [29].

Computed points K (r mm, α° , z mm)	Analytical model in this paper	Double integration model [29]
(1, 30°, 1)	$2.075341353118272e + 03$	$2.075342030279546e + 03$
(2, 60°, 1)	$6.883383752352425e + 03$	$6.883383655587118e + 03$
(2, 90°, 2)	10000	10000 when the integration increment increased to square root of the minimum; indefinite with the minimum integration increment
(3, 60°, 2)	$-9.414782387941905e + 02$	$-9.414783284170040e + 02$
(7, 45°, 3)	$-1.249742783341035e + 02$	$-1.249742322552511e + 02$
(8, 45°, 2)	-97.645377896016626	-97.645374376110695
(9, 0°, 3)	-91.127178430913247	-91.127228807875156

Table 7. Comparison of the radial component of the magnetic field computed by the analytical model derived in this paper and those of double integration form [29].

Computed points K (r mm, α° , z mm)	Analytical model in this paper	Double integration model [29]
(1, 30°, 1)	$3.254215441314990e + 03$	$3.254090873644084e + 03$
(2, 60°, 1)	$5.171522650531067e + 03$	$5.170893368858451e + 03$
(2, 90°, 2)	$6.548622537747931e + 03$	$6.547984542927014e + 03$
(3, 60°, 2)	$2.665756882192566e + 03$	$2.666260855598413e + 03$
(7, 45°, 3)	$1.951738642613515e + 02$	$1.951864669091654e + 02$
(8, 45°, 2)	$1.772092192324710e + 02$	$1.772204783074605e + 02$
(9, 0°, 3)	0	$-5.507071531793312e - 14$ when the integration increment increased to square root of the minimum; indefinite with the minimum integration increment

of the finite-element solver [22]. The average errors of these components drop below 1.5% for the field points in the air space and it keeps decreasing with the increase of the radial distances. On the other hand, using the model by Caciagli et al. [22] produces a minimum error of 24.04% for the azimuthal component and 2.6% for radial component and they go up for the other field points both inside the magnet and in the air space. The inaccuracy of the model by Caciagli et al. [22] can be explained, as in the derivation steps the magnetic scalar potential was approximately presented with the complete elliptic integrals. Then, the final expressions were derived by taking derivatives of this scalar potential

directly, which causes the error when using them to compute the magnetic field. Table 3 presents more details about the maximum, average and minimum errors of the analytical model derived in this paper and those by Caciagli et al. [22].

Evaluated in MATLAB R2016b with the minimum integration increment (double precision in MATLAB), using the analytical expression derived in this paper, it took an average of 4.6 milliseconds on a personal computer (with Processor Intel®Core™i7-6700 CPU @ 3.40 GHz 3.40 GHz) to calculate the axial component at a single location (2000 samples with random input variables). It took less than 0.2 seconds to compute the azimuthal and radial components. On the other hand, using the analytical model by Caciagli et al. [22] in the same configuration, it took 0.08 milliseconds to calculate the axial component and less than 0.02 seconds to compute the azimuthal and radial components. Even though Caciagli’s analytical model computes slightly faster than the presented work in this paper, the results of the presented work are far more accurate. Evaluated in MATLAB with the same configuration as above mentioned, the double integration of the axial component (from Eq. (2)) took 0.33 seconds, the double integration of the azimuthal component took 0.045 seconds and the double integration of the radial component took 0.24 seconds (Table 4). This can demonstrate that the analytical model derived in this study outperforms the double integration expression [29] in terms of the computational cost but very close in terms of the calculated results in most of the randomly selected points (Tables 5, 6 and 7).

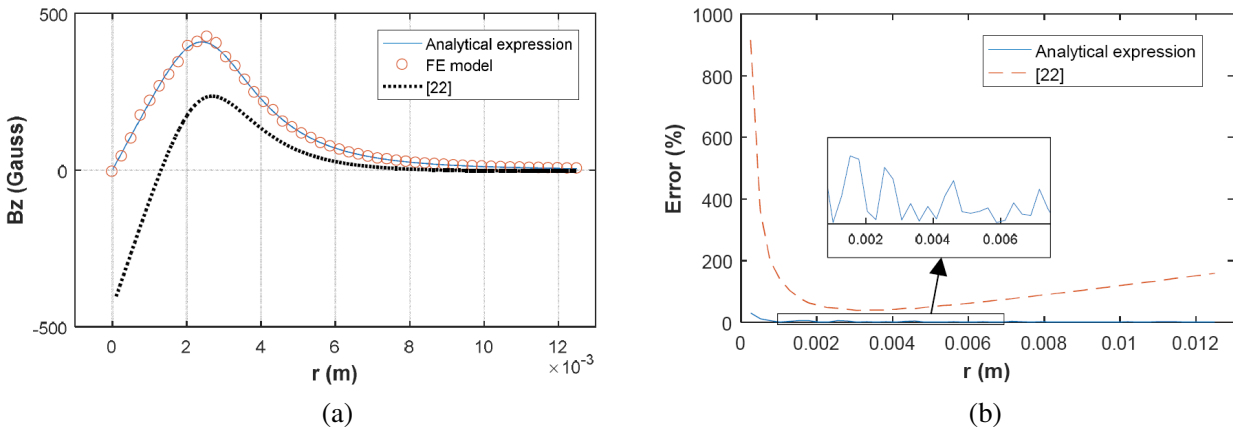


Figure 3. Axial component of the magnetic field: (a) Magnetic field; (b) Error between the analytical models and the FE model.

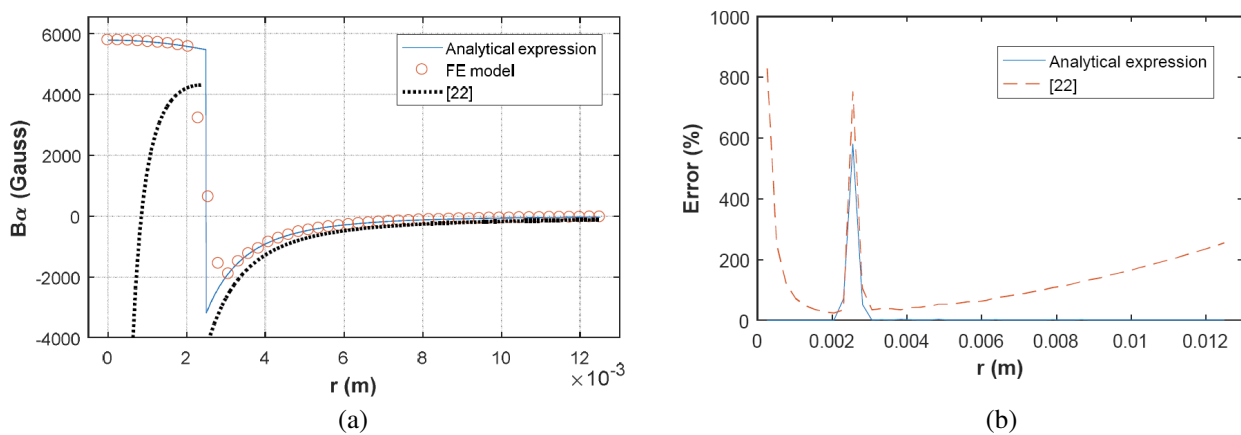


Figure 4. Azimuthal component of the magnetic field: (a) Magnetic field; (b) Error between the analytical models and the FE model.

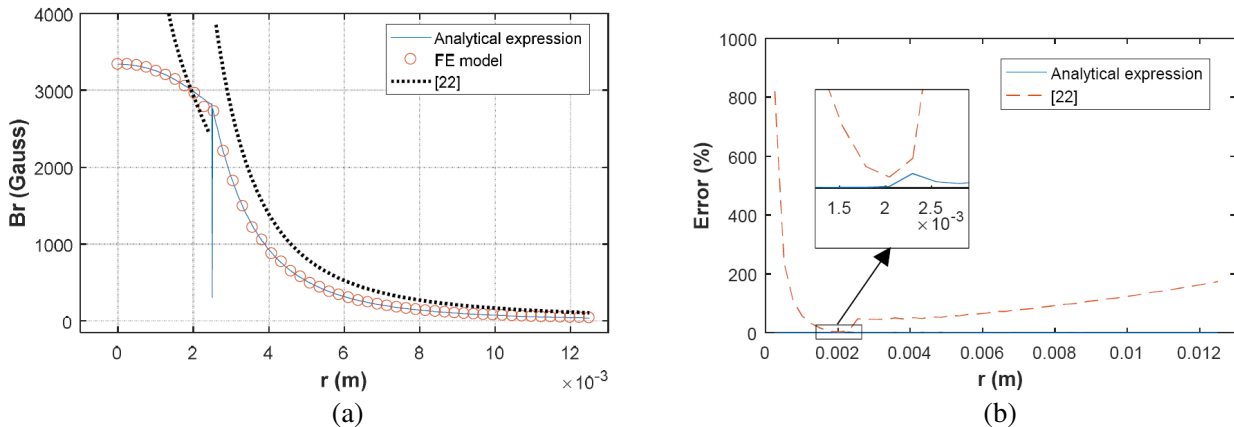


Figure 5. Radial component of the magnetic field: (a) Magnetic field; (b) Error between the analytical models and the FE model.

4. CONCLUSION

An exact analytical model to compute the magnetic field generated by a diametrically magnetised cylindrical/ring shaped permanent magnet with a limited length, at any point in 3D space both inside the magnet and in the air, is presented in this article. Based on geometrical and analytical analyses, without any approximation in the derivation steps, the magnetic field is expressed analytically using the complete elliptic integrals for its axial component and incomplete elliptic integrals for its azimuthal and radial components. The total computational cost of the analytical model is lower than that of double integration model while the two models are in very good agreement in terms of computed results. The results of the developed analytical expressions are in good agreement with those using Finite Element Analysis and far more precise than those obtained by Caciagli et al. [22].

ACKNOWLEDGMENT

The authors are grateful to the EMWORKS Company for providing the license for the EMS software to conduct the Finite Element Analyses. The author would also like to thank the School of Mechanical Engineering, University of Adelaide, Australia, for providing the equipment, facilities and assistance for this research.

REFERENCES

1. Ravaud, R., G. Lemarquand, V. Lemarquand, and C. Depollier, "Permanent magnet couplings: Field and torque three-dimensional expressions based on the Coulombian model," *IEEE Trans. on Magn.*, Vol. 45, No. 4, 1950–1958, Apr. 2009.
2. Cuguat, O., J. Delamare, and G. Reyne, "Magnetic micro-actuators and systems (magmas)," *IEEE Trans. Magn.*, Vol. 39, No. 5, 3607–3612, Sep. 2003.
3. Wang, J., G. W. Jewell, and D. Howe, "Design optimisation and comparison of permanent magnet machines topologies," *Proc. Inst. Elect. Eng.*, Vol. 148, 456–464, 2001.
4. Charpentier, J. F. and G. Lemarquand, "Optimization of unconventional p.m. couplings," *IEEE Trans. Magn.*, Vol. 38, No. 2, 1093–1096, Mar. 2002.
5. Lemarquand, V., J. F. Charpentier, and G. Lemarquand, "Nonsinusoidal torque of permanent-magnet couplings," *IEEE Trans. Magn.*, Vol. 35, No. 5, 4200–4205, Sep. 1999.
6. Berkouk, M., V. Lemarquand, and G. Lemarquand, "Analytical calculation of ironless loudspeaker motors," *IEEE Trans. Magn.*, Vol. 37, No. 2, 1011–1014, Mar. 2001.

7. Kwon, O. M., C. Surussavadee, M. Chari, S. Salon, and K. Vasubramaniam, "Analysis of the far field of permanent magnet motors and effects of geometric asymmetries and unbalance in magnet design," *IEEE Trans. Magn.*, Vol. 40, No. 3, 435–442, May 2004.
8. Paperno, E., I. Sasada, and E. Leonovich, "A new method for magnetic position and orientation tracking," *IEEE Trans. Magn.*, Vol. 37, No. 4, 1938–1940, Jul. 2001.
9. Fountain, T. W. R., P. V. Kailat, and J. J. Abbott, "Wireless control of magnetic helical microrobots using a rotating-permanent-magnet manipulator," *Proc. IEEE Int. Conf. Robot. Autom.*, 576–581, 2010.
10. Wu, S.-T., J.-Y. Chen, and S.-H. Wu, "A rotary encoder with an eccentrically mounted ring magnet," *IEEE Trans. Instrum. Meas.*, Vol. 63, No. 8, 1907–1915, Aug. 2014.
11. Ng, K., Z. Q. Zhu, and D. Howe, "Open-circuit field distribution in a brushless motor with diametrically magnetised PM rotor, accounting for slotting and eddy current effects," *IEEE Trans. on Magn.*, Vol. 32, No. 5, 5070–5072, 1996.
12. Eid, G. and A. Mouillet, "Transistorized dc brushless micromotor with rare-earth permanent magnets," *Proc. Int. Conf. on Electr. Mach.*, 570–573, 1984.
13. Jang, S. M., M. M. Koo, Y. S. Park, J. Y. Choi, and S. H. Lee, "Characteristic analysis on permanent magnet synchronous machines with three types of diametrically magnetized rotors under magnetic circuit construction conditions," *Proc. IEEE Vehi. Power and Prop. Conf.*, 227–230, 2012.
14. Jang, S. M., J. Y. Choi, D. J. You, and H. S. Yang, "Electromagnetic analysis of high speed machines with diametrically magnetized rotor considering slotting effect and applied to new magnetization modelling," *Proc. IEEE Int. Conf. on Electr. Mach. and Driv.*, 1204–1211, 2005.
15. Lemarquand, G. and V. Lemarquand, "Annular magnet position sensor," *IEEE Trans. on Magn.*, Vol. 26, No. 5, 2041–2043, 1990.
16. Smirnov, Y., T. Kozina, E. Yurasova, and A. Sokolov, "Analog-to-Digital converters of the components of a displacement with the use of microelectronic sine-cosine magnetic encoders," *Measurement Techniques*, Vol. 57, 41–46, 2014.
17. Lenzo, B., M. Fontana, S. Marcheschi, F. Salsedo, A. Frisoli, and M. Bergamasco, "Trackhold: A novel passive arm-support device," *ASME J. Mechan. and Robo.*, Vol. 8, 1–9, 2015
18. Wang, S., J. Jin, T. Li, and G. Liu, "High-accuracy magnetic rotary encoder," *System Simulation and Scientific Computing*, 74–82, 2012.
19. Nguyen, V. T., T.-F. Lu, and P. Grimshaw, "Human intention recognition based on contact-less sensors to control an elbow and forearm assistive exoskeleton," *Proc. Int. Conf. Asi. Soc. for Prec. Engin. and Nano. (ASPEN 2017)*, Nov. 2017.
20. Schaller, V., U. Kråling, C. Rusu, K. Petersson, J. Wipenmyr, A. Krozer, G. Wahnström, A. Sanz-Velasco, P. Enoksson, and C. Johansson, "Motion of nanometer sized magnetic particles in a magnetic field gradient," *J. Appl. Phys.*, Vol. 104, 093918, 2008.
21. Warnke, K., "Finite-element modelling of the separation of magnetic microparticles in fluid," *IEEE Trans. Magn.*, Vol. 39, No. 3, 1771–1777, May 2003.
22. Caciagli, A., R. J. Baars, A. P. Philipse, and B. W. M. Kuipers, "Exact expression for the magnetic field of a finite cylinder with arbitrary uniform magnetization," *J. Mag. and Mag. Mater.*, Vol. 456, 423–432, Jun. 2018.
23. Robertson, W., B. Cazzolato, and A. Zander, "A simplified force equation for coaxial cylindrical magnets and thin coils," *IEEE Trans. on Magn.*, Vol. 47, No. 8, 2045–2049, 2011.
24. Ravaud, R., G. Lemarquand, V. Lemarquand, and C. Depollier, "Analytical calculation of the magnetic field created by permanent-magnet rings," *IEEE Trans. on Magn.*, Vol. 44, No. 8, 1982–1989, 2008.
25. Ravaud, R., G. Lemarquand, V. Lemarquand, and C. Depollier, "The three exact components of the magnetic field created by a radially magnetized tile permanent magnet," *Progress In Electromagnetics Research*, Vol. 88, 307–319, 2008.
26. Stratton, J., *Electromagnetic theory*, McGraw-Hill Book Company, New York and London, 1941.

27. Oberteuffer, J., "Magnetic separation: a review of principles, devices, and applications," *IEEE Trans. Magn.*, Vol. 10, No. 2, 223–238, 1974.
28. Wysin, G., "Demagnetization fields," available on <https://www.phys.ksu.edu/personal/wysin/notes/demag.pdf>.
29. Fontana, M., F. Salsedo, and M. Bergamasco, "Novel magnetic sensing approach with improved linearity," *Sensors*, No. 6, 7618–7632, 2013.
30. Furlani, E. P., *Permanent Magnet and Electromechanical Devices: Materials, Analysis and Applications*, Academic Press, 2001.
31. Rakotoarison, H. L., J. P. Yonnet, and B. Delinchant, "Using Coulombian approach for modeling scalar potential and magnetic field of a permanent magnet with radial polarization," *IEEE Trans. on Magn.*, Vol. 43, No. 4, 1261–1264, 2007.
32. Ravaud, R. and G. Lemarquand, "Comparison of the Coulombian and Amperian current models for calculating the magnetic field produced by radially magnetized arc-shaped permanent magnets," *Progress In Electromagnetics Research*, Vol. 95, 309–327, 2009.
33. Babic, S. I. and C. Akyel, "Improvement in the analytical calculation of the magnetic field produced by permanent magnet rings," *Progress in Electromagnetics Research C*, Vol. 5, 71–82, 2008.
34. Ravaud, R., G. Lemarquand, V. Lemarquand, and C. Depollier, "Magnetic field produced by a tile permanent magnet whose polarization is both uniform and tangential," *Progress In Electromagnetics Research B*, Vol. 13, 1–20, 2009.
35. Ravaud, R. and G. Lemarquand, "Analytical expression of the magnetic field created by tile permanent magnets tangentially magnetized and radial currents in massive disks," *Progress In Electromagnetics Research B*, Vol. 13, 309–328, 2009.
36. Fukushima, T., "Precise, compact, and fast computation of complete elliptic integrals by piecewise minimax rational function approximation," *J. Comp. Appl. Math.*, Vol. 282, 71–76, 2015.
37. Fukushima, T., "Fast computation of incomplete elliptic integral of first kind by half argument transformation," *Numer. Math.*, Vol. 116, 687–719, 2010.
38. Fukushima, T., "Precise and fast computation of a general incomplete elliptic integral of second kind by half and double argument transformations," *J. Comp. Appl. Math.*, Vol. 235, 4140–4148, 2011.
39. Fukushima, T., "Precise and fast computation of a general incomplete elliptic integral of third kind by half and double argument transformations," *J. Comput. Appl. Math.*, Vol. 236, 1961–1975, 2012.